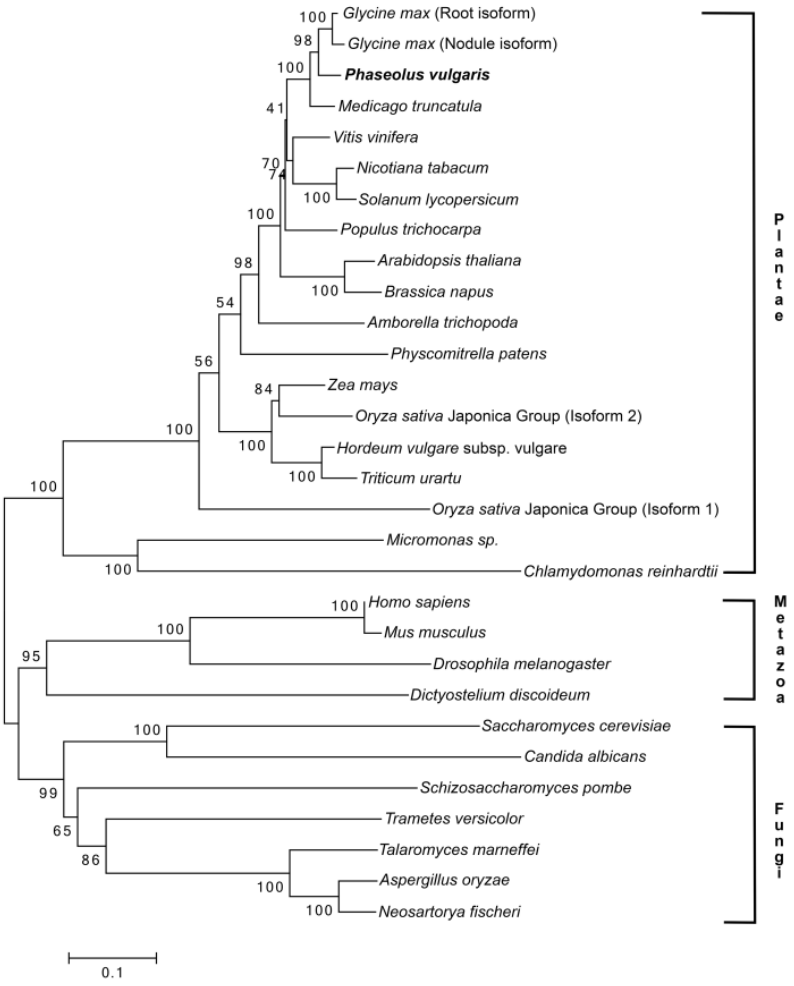

Supplemental Figure 1. Phylogenetic tree of *PI3K* class III proteins.

A phylogenetic tree of PI3Ks was generated from a ClustalW alignment (available as Supplemental Data Set 1) using MEGA7.0. *Phaseolus vulgaris* is in bold. Kindoms are indicated on the right. Numbers represent bootstrap values obtained from 1000 trials (iterations). The scale on the x-axis represents the estimated branch lengths and the numbers indicate bootstrap values. Accession numbers are indicated in the Methods section.

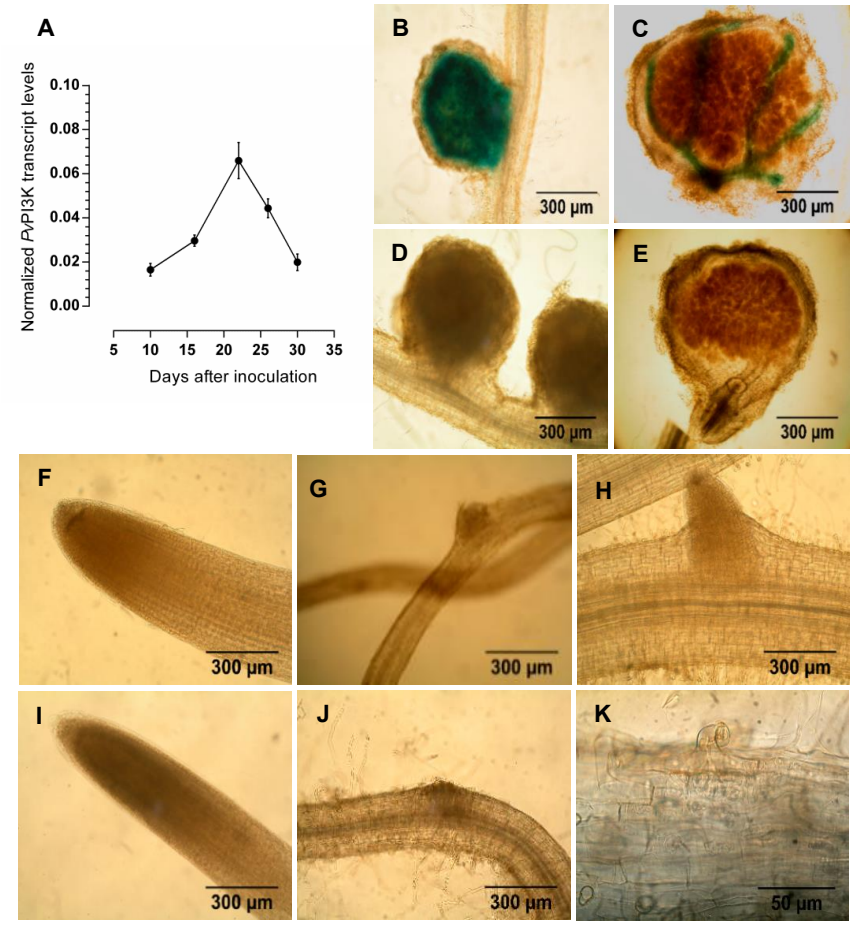
A
Normalized PvPI3K transcript levels
0.10
0.08
0.06
0.04
0.02
0.00
5
10
15
20
25
30
35
Days after inoculation
B
300 µm
C
300 µm
D
300 µm
E
300 µm
F
300 µm
G
300 µm
H
300 µm
I
300 µm
J
300 µm
K
50 µm

Supplemental Figure 2. Pv-*PI3K* transcript levels during nodule development and tissue-specific activity of the Pv-*PI3K* promoter in mature and senescent nodules.

(A) Pv-*PI3K* transcript levels increase as the wild-type *P. vulgaris* nodule reaches maturity, and then decrease as the nodule undergoes senescence. RNA was extracted from nodules harvested from roots at 10, 16, 22, 26, or 30 dai with *R. tropici* CIAT899. Transcript levels were quantified by reverse transcription and real-time PCR (RT-qPCR). Pv-*PI3K* transcript levels were calculated as described in Methods. Normalization calculated using levels of *Elongation Factor 1*α as reference gene. Bars indicate mean ±SD of two independent biological replicates (n = 2 from pool of 10 roots). Statistical significance was confirmed by unpaired two-tailed Student's t-test and is indicated as *, $P < 0.05$; **, $P < 0.01$; or ***, $P < 0.001$.

(B) and **(C)** *PvPI3K*$_{pro}$*:GFP-GUS* activity was detected in the central tissue of a 22 dai mature nodule **(B)**. In the senescent nodule, Pv-*PI3K* promoter activity seems to be restricted to the nodule vascular tissue **(C)**. Promoter activity was revealed by GUS staining of transgenic roots.

(D) to **(K)** No GUS activity was detected in nodules **(D)** and **(E)** and in transgenic roots bearing a promoter-less GFP-GUS construct as a control **(F)** to **(K)**. **(D)**, mature nodule (22 dai); **(E)**, senescent nodule (30 dai). Uninoculated transgenic roots**:** **(F)**, root tip; **(G)** and **(H)**, lateral root primordia. Rhizobia-inoculated roots: **(I)**, root tip; **(J)** early nodule primordium; **(K)** a higher magnification of the nodule primordium shown in **(J)**. Scale bars = 300 µm in **(D)** to **(J)**, and 50 µm in **(K)**.

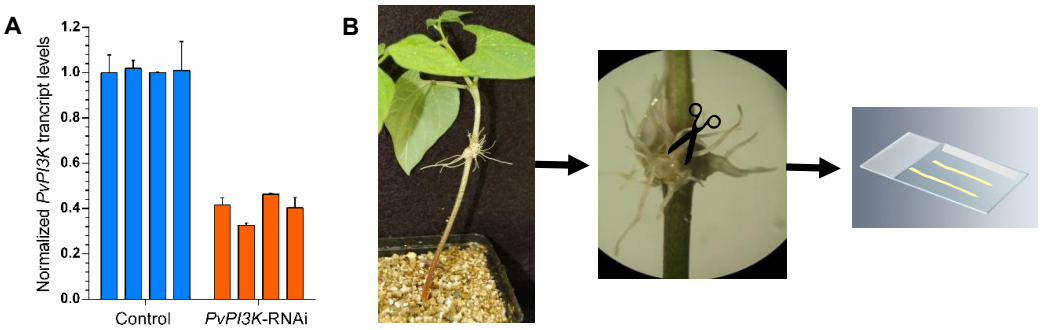

Supplemental Figure 3. Quantification of Pv-*PI3K* transcript levels in individual *PvPI3K*-RNAi transgenic roots.

(A) An approximately 60% decrease in Pv-*PI3K* transcript levels was reproducibly detected in individual *PvPI3K*-RNAi transgenic roots compared to control (TdT-*Sac*-RNAi) roots. Transcript levels were quantified by RT-qPCR and normalized values were calculated based on levels of *Elongation Factor 1*α as reference gene. Pv-*PI3K* transcript levels were calculated as described in Methods. Each sample was assessed in triplicate and the mean was plotted as an independent bar. Error bars indicate standard deviation (± SD).

(B) Serial images showing the procedure used to mount sections (3 cm) of young transgenic roots on glass microscope slides for microscopy analysis of the root hair phenotype.

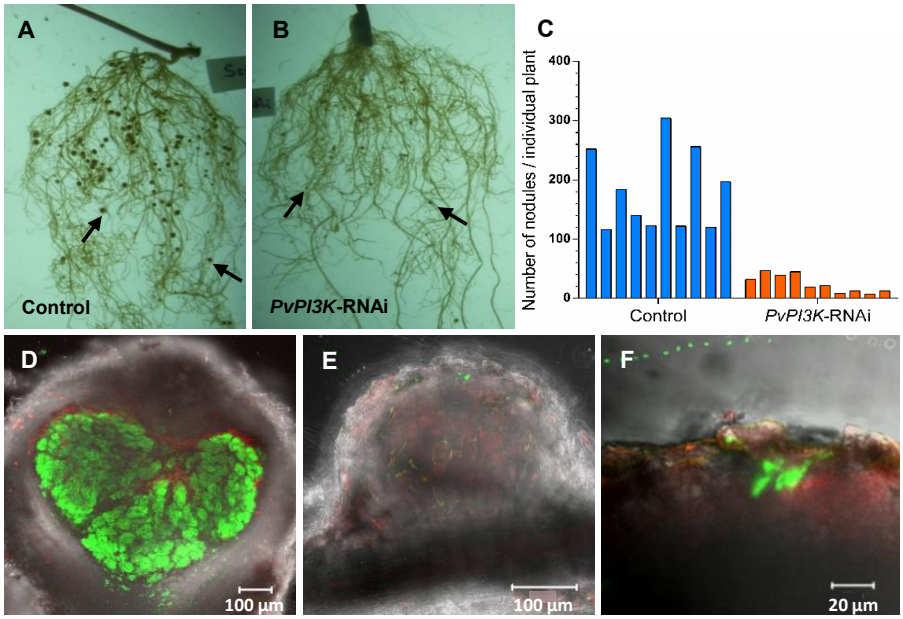

Supplemental Figure 4. Loss-of-function of Pv-*PI3K* led to a reduction in *P. vulgaris* nodule number and impaired root nodule development.

(A) Images of whole nodulated roots (22 dai) showing a decrease in the number of nodules in *PvPI3K*-RNAi transgenic roots in **(B)** with respect to control (TdT-*Sac*-RNAi) transgenic roots **(A).** Arrows indicate representative nodules.

(C) Individual *PvPI3K*-RNAi transgenic roots had fewer nodules per plant (24.50± 14.39) than did control transgenic roots (172.40 ± 68.50) at 22 dai. *n* = 10 roots from composite plants.

(D), **(E),** and **(F)** Representative *in vivo* images of nodules harvested at 17 dai from TdT-*Sac*-RNAi control **(D)** and *PvPI3K*-RNAi transgenic roots **(E)** and **(F),** taken by laser scanning confocal microscopy. Nodules were harvested from transgenic roots infected with *R. tropici* CIAT899 expressing GFP and hand-sectioned to determine whether the central tissue of the nodule had infected cells (green fluorescence). **(D)** Nodule from TdT-*Sac*-RNAi control transgenic root containing infected cells. **(E)** Small nodule, representative of those observed in *PvPI3K*-RNAi transgenic roots. No infected cells were detected in the central tissue. **(F)** Higher magnification (63x) of an abortive IT in the periphery of the nodule shown in **(E)**.

Images were acquired *in vivo* using a Zeiss LSM 510 Meta Confocal Microscope; 18 optical sections each of 18.0 μm were acquired for the control (magnification 10x) in **(D),** whereas 12 optical sections each of 10 μm (magnification 20x) **(E)** and 29 optical sections each of 1.0 μm (magnification 63x) **(F)** were acquired for *PvPI3K*-RNAi transgenic roots**.** Scale bar = 100 μm in **(D)** and **(E)** and 20 μm in **(F)**.

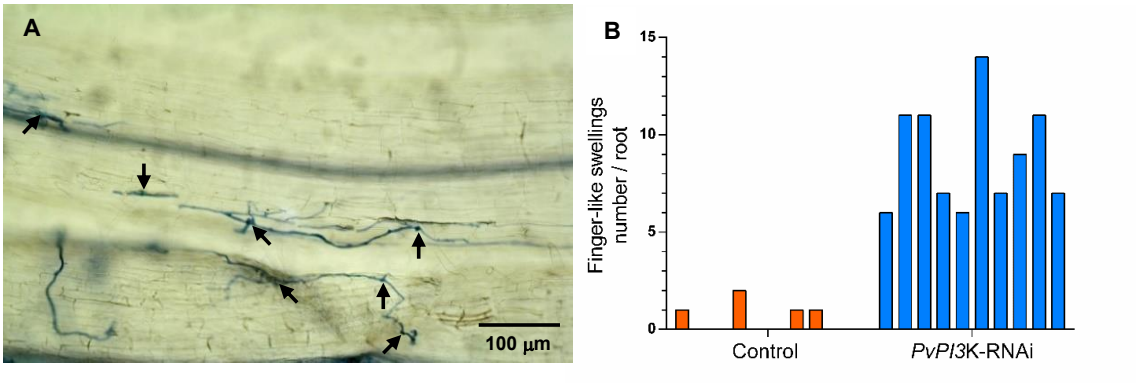

Supplemental Figure 5. Extraradical hyphae growth and finger-like swellings are increased after *R. irregularis* inoculation in *PvPI3K* loss-of-function of *P. vulgaris* roots.

(A) Image of *PvPI3K*-RNAi transgenic root infected with *R. irregularis* and stained with trypan blue, showing hyphae that failed to penetrate the root epidermis. Finger-like swellings or outgrowths are highlighted by arrows.

(B) Finger-like swellings are numerous in *R. irregularis*-inoculated *PvPI3K*-RNAi roots compared with control transgenic roots expressing TdT-*Sac*-RNAi. Quantitative analysis of finger-like swellings in individual transgenic roots (n = 10), based on three independent experiments.

Supplemental Table 1. Oligonucleotides used in this study

Name	Oligonucleotide sequence (5`-- 3`)
For quantitative PCR (qPCR)	
*PvPI3K*q_F	GGC AGC TGG TGT GAA TGG AGA G
*PvPI3K*q_R	CAA CTG AGC TGT CAA TTC AGT CTG G
*PvVps*15q_F	GCA AGC AAG AGA ATA CTG CCA AGA G
*PvVps*15q_R	GCT ATG CCT CTT CTC TAG CAT CAG G
*PvBeclin1*q_F	CTG CCG CAA TCC TCT CTG CAT C
*PvBeclin1*q_R	CAC ACT GCT GGC ACC ATG AAC G
*PvAtg8*q_F	TCC CTG CTG ACC TGA CTA TTG G
*PvAtg8*q_R	TGT AGG AGG AAG GAC GTT GTC C
PvEF1α q_F	GGT CAT TGG TCA TGT CGA CTC TGG
*PvEF1α*q_R	GCA CCC AGG CAT ACT TGA ATG ACC
*PvENOD40*q_F	AGT TTT GTT GGC AAG CAT CC
*PvENOD40*q_R	TAA GCA CAA GCA AAC TGT TG
*PvPT-4*q_F	GCG GTG ACT AAC ATG TTA GGG
*PvPT-4*q_R	CCT GTG CCC TAG TAT TGT TGG
For PI3K probe	
*PI3K*_F	GAA AGA GCT GAT GAT GAA GA
*PI3K*_R	GCA CAG CTT TTT ATA AAT GT
For Gateway cloning	
PvPI3K$_{pro}$_F	CAC CAT GTA TGA TAG ATA TGT TAT TGG
PvPI3K$_{pro}$_R	GAT CAG ATC TTT GGA ACT ACT TCT TTG TAC TG
PvPI3K-RNAi_F	CAC CAG AGC ATC GTA GCA TCAT AAG C
PvPI3K-RNAi_R	CCA TCT GAG GGA ATA ATG CAC TC
Pv*Beclin1*-RNAi_F	CAC CAT GCA AGG GTC GTC CGT TCA TG
Pv*Beclin1*_RNAi_R	CAA CCT CTT TAT CAA GTT TAT CTG AC
Wrky-3_F	CTT CTC CAA CCA CAG GAA TTC ATC
Wrky-5_R	GCA GAG GAG GAG AAG CTT CTA G

Supplemental Table 2. Quantification of root hairs and curling in loss-of-function of *PvPI3K* and control *P. vulgaris* roots.

	Un-inoculated		Root-hairs (%)		
	hairy-roots	analyzed fields	length > 130 μm	length < 130 μm	bulges
Control	16	234	33.12 ± 4.36	51.56 ± 3.20	15.37 ± 2.31
PvPI3K-RNAi	15	293	14.36 ± 2.60	56.93 ± 4.31	28.86 ± 4.69

	Inoculated		Root-hairs (%)	
	hairy-roots	analyzed fields	Non-curled	Curled
Control	16	191	68.70 ± 3.90	31.30 ± 4.20
PvPI3K-RNAi	15	293	96.60 ± 8.00	3.39 ± 1.70

Distribution of root hair lengths analyzed using a Zeiss Axiovert 200M microscope (Normarski optics) and counted (%) in the visual field / mm (analyzed fields) along the hairy roots. For *PvPI3K*-RNAi un-inoculated roots; root hairs > 130 μm, ($P<0.001$); root hairs < 130 μm, (ns, non significant) and bulges ($P<0.009$; n=15). For *PvPI3K*-RNAi inoculated roots; curled root hair ($P<0.05$; n=15). Values are mean (%) ±SEM and statistical significance differences were determined using an unpaired two-tailed Student´s *t*-test with Welch´s correction.